

THE BACKGROUND, TECHNICAL DEVELOPMENT, AND TESTING OF TRAJECTORY ANALYSES TO IDENTIFY SECONDARY-TO-SOURCE IMPACT CRATER RELATIONSHIPS. J.A. Skinner, Jr.¹, J.R. Laura^{1,2}, C.M. Fortezzo¹, J. Hagerty¹, and T.M. Hare¹, ¹Astrogeology Science Center, U.S. Geological Survey, 2255 N. Gemini Dr., Flagstaff, AZ 86001; ²School of Geographical Sciences and Urban Planning, Arizona State University, 975 S. Myrtle Ave., Tempe, AZ 85287, (jskinner@usgs.gov).

Introduction: The majority of crater clusters on rocky bodies of the inner Solar System are interpreted to have resulted from end member scenarios: atmospheric breakup of weak, stony meteoroids or the high-velocity ejection of large blocks from the surface as secondary debris from primary impacts [1-4]. The morphometry of the resultant debris field varies based on the size of the target body, the rigidity of the target material, and the angle of the impactor with regard to the planetary surface [4]. Herein, we present the rationale, technical development, and testing of an analytical method that uses large crater clusters (LCCs) to identify potential source craters on rocky bodies where clusters can be mapped with locational confidence.

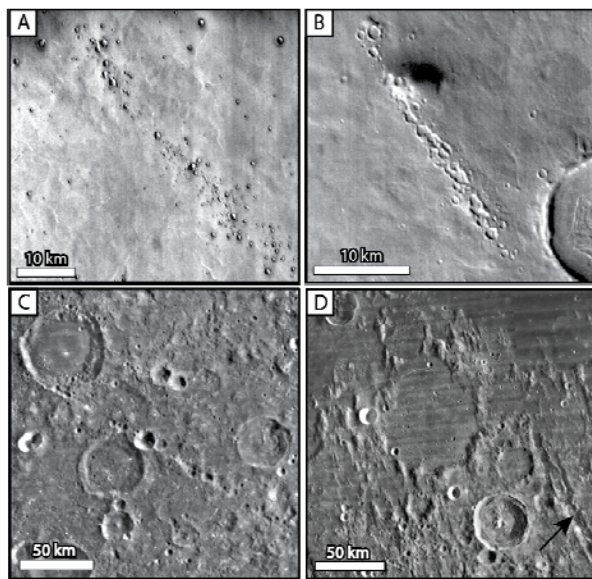


Figure 1. Examples of large secondary crater landforms on the Mars and the Moon. (A) Cluster in W. Utopia Planitia. (B) Cluster north of Nilosyrtis Mensae. (C) Eratosthenian-age Catena Abulfeda located in the lunar highlands west of Mare Nectaris. Source unclear. (D) Pre-Imbrian-age (?) crater Flammarion (center), deformed, surrounded, and superposed by Imbrium ejecta (NW-SE orientations).

Background: Our current research derives from mapping efforts in the Martian northern plains [5]. We noticed local to regional “over-abundances” of small diameter (< 1km) impact craters, indicative of secondary populations [5-6]. Shallow floors, poorly-formed rims, and varying spatial alignment suggest that many of these craters formed either as fragmented primaries or ejected secondaries. We hypothesized that second-

ary-source links could be used to extrapolate temporal relationships across multiple, non-contiguous terrains and yield critical constraints on impact dynamics.

Technical Development: In 2008, we developed a three-step analytical toolset in Visual Basic.NET (named the LCC Analysis Toolset) to be used as a plug-in to the Environmental systems Research Institute (ESRI) ArcGIS 9.3 software package [7-8]. This approach has been refined through ongoing testing (described below). Step 1 provides clustering and directional distribution analyses of “mass mapped” point features. Step 2 calculates trajectories of statistical clusters as great circles. Step 3 identifies statistical clusters of intersected trajectories. The user is prompted for inputs at each step, including nearest neighbor distance for cluster identification, points per cluster, minimum cluster ellipticity, and a counter-effect for the Coriolis force (using average ejecta velocity). The original tool was posted on USGS and ESRI websites in January, 2011.

Though the toolset is analytically effective [7-8], functional limitations have persisted due to incompatibility with subsequent ArcGIS versions, large computational times when using large point data sets, and the inability to use mapped lines in addition to (or instead of) mapped points. As such, we have upgraded the existing toolset through several iterations of development and testing. Current improvements include:

- Increased computational efficiency by indexing nearest neighbor statistics prior to Step 1 analyses;
- Modified clustering and trajectory intersection tools (Steps 1 and 3) using DBScan to increase sensitivity to cluster shape and count;
- Optional “optimization” button for Step 1 and 2 tools to avoid reliance on outputted text files;
- Input of points and polylines as well as compatibility with shapefile and geodatabase formats;
- Use of polyline files in trajectory analyses (Step 2), which allows the user to effectively skip Step 1;
- Optional “save log” with specified location;
- Detailed help documentation as PDF and HTML.

These efforts yield a statistically robust toolset for identifying spatial linkages between secondary crater clusters and related landforms with primary sources.

Performance Testing: Systematically changing input features and toolset parameters provides not only a test of operational effectiveness but also guides subsequent iterations in search of source craters.

Zunil crater (Mars). Secondary craters are prevalent in proximity to larger impact craters; however, spatial relationships for distal populations are prone to over-simplification in identifying sources. Zunil, a 10.1 km diameter, Late Amazonian impact crater in Elysium Planitia, is surrounded by a secondary field [9] that provides exceptional calibration for testing and developing the existing toolset. We mapped >22,000 possible Zunil secondaries using THEMIS VIS images. Mass mapped points served as inputs for multiple program iterations, each of which calculated and displayed the effects that different cluster characteristics, ejection velocities, and angular rotations have on the modeled location of the source crater. Results, presented in [7], indicate: (1) optimized parameters identify the source as a point located < 2.0 km from Zunil's actual center, (2) distance between modeled and actual source center decreases with increasing cluster ellipticity, (3) human- and auto-identified clusters identify comparable source locations, though with differing parameters, (4) inclusion of rotational velocities to account for the Coriolis effect has varying effects on accurately correlating modeled and actual source location, and (5) some mapped secondaries do not appear to source from Zunil crater. Though Zunil secondaries have smaller diameters than those that define LCCs, these tests are invaluable for improving the toolset.

Lyot crater (Mars). The parameter space defined by the Zunil tests establish a baseline for application to other regions of Mars where the source crater is truly unknown. We have used a dense field of LCCs in SW Utopia Planitia, which we consider to be representative of LCCs due to their ellipticity, area, and density. Some of these craters have been suggested to originate from Lyot crater [10], located in the Martian mid-latitudes along the Martian dichotomy boundary. We find that some of the auto- and manually-identified LCCs in the region can be confidently tracked to Lyot crater (D=221.5 km), though there are many more that do not, suggesting secondary-source linkage requires a more robust approach using the existing toolset. This may include manual mapping LCCs as points and lines using base maps that capture the target population.

Impact craters (Moon). For simple to complex lunar craters, we used clusters and rays around Copernicus crater, which has long served as a referent for the lunar time-stratigraphic system. We mapped 35 clusters located in mare units around Copernicus crater as points using the Lunar Orbiter Clementine (750 nm) "blended" mosaic. These included clusters within bright rays located between Copernicus and both Aristarchus and Kepler craters (as a means to assess the tool's ability to resolve different source regions). In addition, we mapped several clusters that display key

cross-cutting relationships with surrounding landforms, such as Euler crater. Using "optimized" parameters, the toolset identified a first-rank source as a location 24 km from the true center of Copernicus. Several modeled trajectories intersected both Aristarchus and Kepler craters, illustrating first-order ability to partition overlapping clusters.

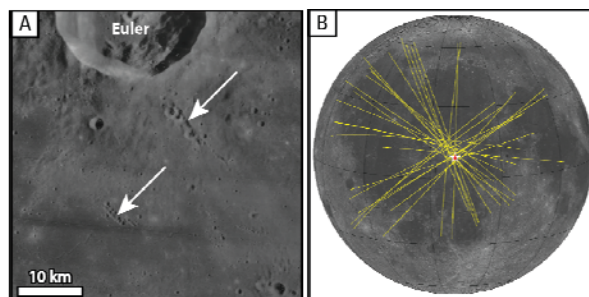


Figure 2. Examples of secondary-source relationships on the Moon. (A) Clusters and catenae identified in base images. (B) Projected source location estimated by trajectory intersections (red star), which is located 24 km from Copernicus.

Impact basins (Moon). To examine our ability to identify lunar impact basins, we mapped the dominant orientations of 59 highland features – lineations (n=39) and catenae (n=20) – located on various terrains on the lunar near-side. Optimized parameters resulted in the identification of Imbrium, Orientale, and Humorum as first-, second-, and third-rank source regions, respectively. These tests illustrate (1) the tool not only works for features at multiple scales but also that statistical ranking capabilities are functional, (2) there are analytical limitations when only using features within certain spatial quadrants, and (3) statistical relationships often require visual examination to establish confidence in results, particularly for very ancient (stratigraphically obscured) lineations and basins.

Acknowledgements: This work was supported by NASA's Lunar Advanced Science and Exploration Research (LASER) Program and Mars Data Analysis Program (MDAP) under award Nos. NNH12AU54I and NNH09AM15I, respectively (PI Skinner).

References: [1] Hartmann, W.K. (1969) *Icarus*, 10, 201-213. [2] Holsapple, K.A. and Schmidt, R.M. (1982) *JGR*, 87, 1849-1870. [3] Vickery, A.M. (1986) *Icarus*, 67, 224-236. [4] Popova, O.P., et al. (2007), *Icarus*, 190, 50-73. [5] Tanaka, K.L. et al. (2005), *USGS SIM* 2888. [6] Robbins, S.J. and B.M. Hynek (2011), *JGR*, 116, E10003. [7] Nava, R.A. and Skinner, J.A., Jr. (2009) *AGU Fall Suppl.*, P23A-1243. [8] Nava, R.A. and Skinner, J.A., Jr. (2010) *LPS XLI*, Abstract #2699. [9] Preblich, S. et al. (2007) *JGR*, 112. [10] Robbins, S.J. and B.M. Hynek (2011) *GRL*, 38, L05201.